

ГОДИШНИК НА УНИВЕРСИТЕТА ПО АРХИТЕКТУРА, СТРОИТЕЛСТВО И ГЕОДЕЗИЯ – СОФИЯ

Юбилейна приложна научно-техническа конференция
„65 години Хидротехнически факултет и 15 години немскоезиково обучение”

6–7 ноември 2014
6–7 November 2014

International Jubilee Conference
„65th Anniversary Faculty of Hydraulic Engineering and 15th Anniversary Hydraulic Engineering in German”

ANNUAL OF THE UNIVERSITY OF ARCHITECTURE, CIVIL ENGINEERING AND GEODESY – SOFIA

XLVII ^{TOM}
vol.

2014

св.
fasc. I-B

FERRIMAGNETIC NANOPARTICLES FOR SELF-CONTROLLED MAGNETIC HYPERTHERMIA (PHYSICAL ASPECTS)

A. Apostolov¹, I. N. Apostolova²

Keywords: ferrites nanoparticles; magnetic hyperthermia

Research area: physical science; solid state physics

ABSTRACT

Based on the Heisenberg model including single-site uniaxial anisotropy and using a Green's function technique we studied the influence of size and composition effects on the Curie temperature T_C , saturation magnetization M_S and coercivity H_C of spherical nanoparticles with a structural formula $Me_{1-x}Zn_xFe_2O_4$, $Me = Ni, Cu, Co, Mn$. It is shown that for $x = 0.4 - 0.5$ and $d = 10 - 20$ nm these nanoparticles have a $T_C = 315$ K and are suitable for a self-controlled magnetic hyperthermia.

1. Introduction

Magnetic hyperthermia (MHT) is the most promising method in cancer treatment because of its capability to destroy the tumor cells selectively by heating them up to a desired temperature range (e.g. $42^\circ - 46^\circ$ °C) at which the healthy tissues can still survive. In selecting nanoparticle (NPs) for hyperthermia treatment is essential to find those with the highest specific heat absorption rate value.

The NPs suitable for application in MHT must satisfy the following requirements: (i) a Curie temperature T_C around $42^\circ - 46^\circ$ °C (temperatures above that may cause necrosis); (ii) a large saturation magnetization M_S , so that to show a large response by applying a magnetic

¹ Angel Apostolov, Assoc. Prof. Dr., Dpt. “Physics”, UACEG, 1 H. Smirnenski Blvd., Sofia 1046, e-mail: angelapos@abv.bg

² Iliana Apostolova, Assoc. Prof. Dr., Dpt. “Mathematics and Physics”, University of Forestry, 10 Kliment Ohridski Blvd., Sofia 1756, e-mail: inaapos@abv.bg

field; (iii) a low coercive field H_C ; (iv) a limiting size case of the order of 20 – 25 nm for *in vivo* applications; and (v) bio-compatibility.

In the last years intensively are investigated experimentally the magnetic properties of Zn doped CoFe_2O_4 [1], NiFe_2O_4 [2], CuFe_2O_4 [3] NPs and MnFe_2O_4 [4].

The aim of the present paper is to extend our results from [5] and to investigate different Zn doped ferrite NPs, such as Co, Cu and Ni ferrite, in order to find an appropriate T_C for application in MHT. For Zn-Ni, Zn-Co and Zn-Cu ferrites we have a mixed ferrimagnetic spin system. The magnetic ions have different spin values. This requires the definition of six types exchange interactions ($\text{Fe}^A\text{-Fe}^A$, $\text{Fe}^A\text{-Fe}^B$, $\text{Fe}^A\text{-Me}^B$, $\text{Fe}^B\text{-Fe}^B$, $\text{Fe}^B\text{-Me}^B$ and $\text{Me}^B\text{-Me}^B$) and three magnetic sublattices (Fe^A , Fe^B and Me^B). Numerous experimental data show that the following exchange interactions $\text{Fe}^A\text{-Fe}^B$, $\text{Fe}^A\text{-Me}^B$ and $\text{Fe}^B\text{-Me}^B$ are responsible to the magnetic properties of these compounds.

2. The Model

In $\text{Me}_{1-x}\text{Zn}_x\text{Fe}_2\text{O}_4$ systems Zn^{2+} displaces the Fe^{3+} from a tetrahedral to octahedral site where Fe^{3+} displaces Me^{2+} so that the octahedral sites become poor of Me^{2+} ions with increasing x . The magnetization of sublattice A is decreased by the presence of Zn whereas the magnetization of B sublattice is increased because of the Zn^{2+} magnetic momentum lack. This is true for small amount of Zn^{2+} ions. In this case a collinear ferromagnetic phase exists. However, at higher Zn^{2+} concentration (higher doping levels) the net magnetic moment starts to decrease which can be explained in terms of the non-collinear spin arrangement, i.e. the presence of small canting of the B site moment with respect to the direction of the A site moment. This non-collinearity in the B sublattice is described by the Y-K angles [6] which are responsible for deviation from the Neel model [7]. In Zn doped ferrites the coercivity H_C decreases due to the magneto crystalline anisotropy [8]. The total anisotropy consists of the single ion anisotropies of the Zn and Me ions.

The anisotropy of the Me ion is usually greater compared to that of the Zn ion. Therefore, with the replacement of Me^{2+} by Zn^{2+} ion the magneto crystalline anisotropy decreases leading to H_C reduction. This means that by manipulating the composition of these compounds, doping with Zn ions, we can transform them from hard magnetic to soft magnetic materials. In mixed ferrites the Curie temperature T_C decreases with increase of the Zn^{2+} concentration which can be qualitatively explained by the decrease of the A-B interaction with Zn doping.

From a brief overview of the properties of mixed spinels ($\text{Me}_{1-x}\text{Zn}_x\text{Fe}_2\text{O}_4$) NPs suitable for MTH we can conclude that appropriate Me-Zn NPs are such NPs with Zn concentration in the range of 0 to 50%. For $0 \leq x \leq 0.4 - 0.5$, M_S increases, H_C and T_C decrease, and we have a collinear ferromagnetic arrangement. In a more complicated non-collinear Y-K model [6] the B sublattice is divided into two halves each of them oppositely canted at the same angle (Y-K angle or α_{YK}). On the basis of the Y-K approach experimental and numerical results show that for $0 \leq x \leq 0.4 - 0.5$ the α_{YK} angle is zero or close to zero and when the temperature increases α_{YK} decreases [9]. Therefore, we assume that there is a collinear arrangement of spins in mixed spinels with $0 \leq x \leq 0.4 - 0.5$, i.e. the Neel model could be applied.

The Hamiltonian of the system and the numerical calculations are based on the following assumptions:

(i) The Me-Zn ferrites possess a collinear arrangement of spins in tetrahedral and octahedral sites. The existence of a collinear magnetic structure in Zn ($0 \leq x \leq 0.4 - 0.5$)

doped $MeFe_2O_4$ compounds is experimentally found in [10]. We take into account the collinear structure through the two sublattices A and B (shells in our nanoparticle). (ii) Zn^{2+} displaces iron Fe^{3+} ions only from tetrahedral sites (sublattice A) while Me^{2+} occupies together with Fe^{2+} only octahedral sites (sublattice B). (iii) The undoped ferrites are completely inverse spinels. (iv) The mixed Heisenberg ferrimagnetic model with localized A- and B-site spins is used to describe the magnetic properties. (v) The single-site uniaxial anisotropy for A- and B-sites is included. (vi) The A-A interaction is neglected because it is 10 times weaker than the A-B and B-B interactions. (vii) For certain x in $Me_{1-x}Zn_xFe_2O_4$ the change of one type of Me^{2+} ion does not change the nature of the interaction between the iron ions. In the case of non-magnetic Me^{2+} -ions (for example Mg^{2+} or Li^{1+}) it is possible to determine the value of the A-B interaction between the Fe^{3+} ions. (viii) In the B sublattice we presume that an effective interaction between Fe^{3+} - Me^{2+} will occur, characterizing the ferromagnetic contribution to the B-B interaction

The Hamiltonian which describes the magnetic characteristics of the Me -Zn NPs is:

$$\begin{aligned}
H = & \sum_{ij} J_{ij}(Fe^A - Fe^B) \bar{S}_i(Fe^A) \cdot \bar{S}_j(Fe^B) + \sum_{ij} J_{ij}(Fe^A - Me^B) \bar{S}_i(Fe^A) \cdot \bar{S}_j(Me^B) + \\
& + \sum_{ij} J_{ij}(Fe^B - Me^B) \bar{S}_i(Fe^B) \cdot \bar{S}_j(Me^B) - \sum_i D_i(Me^B) [S_i^z(Me^B)]^2 - \\
& - \sum_i D_i(Fe^B) [S_i^z(Fe^B)]^2 - \sum_i D_i(Fe^A) [S_i^z(Fe^A)]^2 - g_{Me} \mu_B h \sum_i S_i^z(Me^B) - \\
& - g_{Fe} \mu_B h \sum_i [S_i^z(Fe^B) + S_i^z(Fe^A)].
\end{aligned} \tag{1}$$

Here, $S_i(X^\alpha)$ ($\alpha = A, B$ -sublattice and $X = Fe, Me$) is the Heisenberg spin operator at the site i . $J_{ij}(Fe^A - Fe^B)$, $J_{ij}(Fe^A - Me^B)$ and $J_{ij}(Fe^B - Me^B)$ are exchange interaction constants between the A-B and B-B magnetic ions at sites i and j . $D_i(X^\alpha)$ is the single-site anisotropy parameter, $|D| \ll J$. h is an external magnetic field in z -direction. We assume for simplicity only nearest neighbor exchange interaction with the notations: index “ s ” at the surface and “ b ” in the bulk of the NP. We consider spherical NPs, i.e. with a cubooctahedral symmetry. A NP is defined by fixing the origin at a certain spin in the center of the particle and including all spins within the particle into shells. The shells are numbered by $n = 1, \dots, N$, where $n = 1$ denotes the central spin and $n = N$ represents the surface shell of the system.

The Green’s function method still seems probably the most appropriate tool to study complex systems with low symmetry. In contrast to extended materials the Green’s function for small particles has to be formulated in real space. The reason is the local environment, which is the key to understanding the properties of complex systems. Moreover, the real-space Green’s function leads directly to the local density of states. We define the following retarded Green’s function:

$$\begin{aligned}
& \ll S_i^+(Fe^A); S_j^-(Fe^A) \gg_E; \ll S_i^+(Fe^A); S_j^-(Me^B) \gg_E \\
& \ll S_i^+(Me^B); S_j^-(Fe^A) \gg_E; \ll S_i^+(Fe^B); S_j^-(Fe^A) \gg_E \\
& \ll S_i^+(Fe^A); S_j^-(Fe^B) \gg_E; \ll S_i^+(Me^B); S_j^-(Me^B) \gg_E.
\end{aligned} \tag{2}$$

The magnetization of the system is:

$$M = |M^B - M^A| \quad (3)$$

with

$$M^B = \sum_{i,n} \left(\langle S_i^z (Fe^B) \rangle_n + \langle S_i^z (Me^B) \rangle_n \right), \quad M^A = \sum_{i,n} \langle S_i^z (Fe^A) \rangle_n \quad (4)$$

3. Numerical Results and Discussion

As we mentioned above it is well known that after the addition of Zn ions (which are nonmagnetic) to spinel ferrites their magnetization increases with Zn-content, $x \leq 0.4 - 0.5$. We have constructed Table 11 using the experimental data [2 – 4, 6].

The last column of the different compounds is obtained on the basis of the phenomenological Weiss theory of magnetism. Following this theory the relation is valid:

$$J(x) = \text{const} * \frac{T_C(x)}{M^2(x)} \quad (5)$$

From here we can find a connection between the exchange interactions in $MeFe_2O_4$ and $Me_{1-x}Zn_xFe_2O_4$ ferrites:

$$\frac{J(x)}{J(x=0)} = \frac{T_C(x)}{T_C(x=0)} * \frac{M^2(x=0)}{M^2(x)} \quad (6)$$

In order to define the exchange interaction constants we will begin with the $MgFe_2O_4$ compound. It is somewhat simpler than the other spinels since only the Fe^{A3+} - Fe^{B3+} exchange occurs (Mg^{2+} is non-magnetic). This consideration is valid only for the assumptions, made in the previous paragraph. The bulk $MgFe_2O_4$ has a Curie temperature $T_C = 730$ K [42]. On the basis of the molecular field theory it is true the following:

$$k_B T_N = \frac{1}{2\sqrt{3}} (z_A z_B)^{\frac{1}{2}} J (Fe^A - Fe^B) \quad (7)$$

with $z_A = 12$, $z_B = 6$, $S = 5/2$. Then we find:

$$J(Fe^A - Fe^B) = 33.78 \text{ K} \quad (8)$$

Now we consider $CoFe_2O_4$. We will assume that the electron exchange between Co^{2+} and Fe^{3+} ions in the B-sites is so intensive that these sites are effectively occupied by a single ionic species with spin \tilde{S} and effective A-B exchange constant \tilde{J} . The exchange interaction constant J between the Fe^A and Fe^B ions is renormalized through the interaction included in the Hamiltonian between the Fe^A ion with the Co^B ion. It is obvious that \tilde{S} and \tilde{J} can be defined as follows:

$$\tilde{S} = \frac{1}{2} [S(Fe^B) + S(Co^B)], \quad (9)$$

Table 1. The Curie temperature T_C , magnetization M_S and ratio between exchange interaction constants $\Delta Me^B = \frac{J_{Fe^A - Me^B}(x)}{J_{Fe^A - Me^B}(0)}$ in bulk $Me_{1-x}Zn_xFe_2O_4$ ferrites for different Zn-concentrations.

x(Zn)	Mg _{1-x} Zn _x Fe ₂ O ₄			Ni _{1-x} Zn _x Fe ₂ O ₄			Cu _{1-x} Zn _x Fe ₂ O ₄		
	T _C (K)	M _s (μ _B)	Δ _{Me} ^{Mg}	T _C (K)	M _s (μ _B)	Δ _{Me} ^{Ni}	T _C (K)	M _s (μ _B)	Δ _{Me} ^{Cu}
0	730	1,00	1,00	850	2,20	1,00	744	1,20	1,00
0,1	715	2,00	0,49	814	2,92	0,72	716	2,14	0,54
0,2	670	2,80	0,33	750	3,60	0,54	659	3,00	0,35
0,3	630	3,30	0,26	685	4,20	0,42	601	3,80	0,26
0,4	610	3,50	0,24	620	4,80	0,33	542	4,25	0,21
0,5	540	3,30	0,22	560	5,00	0,29	463	4,00	0,19

x(Zn)	Co _{1-x} Zn _x Fe ₂ O ₄			Mn _{1-x} Zn _x Fe ₂ O ₄		
	T _C (K)	M _s (μ _B)	Δ _{Me} ^{Co}	T _C (K)	M _s (μ _B)	Δ _{Me} ^{Mn}
0	728	3,29	1,00	573	4,60	1,00
0,1	663	4,00	0,75	544	5,35	0,82
0,2	613	4,40	0,63	525	5,80	0,73
0,3	558	4,65	0,54	500	6,00	0,67
0,4	488	4,85	0,45	463	6,20	0,60
0,5	403	4,66	0,39	413	6,30	0,53

$$\tilde{J} = \frac{1}{2}[J(Fe^A - Fe^B) + J(Fe^A - Co^B)]. \quad (10)$$

Then from the Curie temperature of CoFe₂O₄ ($T_C = 728$ K) and the molecular field theory we find: $\tilde{J} = 23.26$ K (11)

In this case \tilde{J} is an effective interaction between the A- and B-sublattices and can be obtained on the basis of a Mossbauer study. Clave et al. [11] by a fitting procedure from Mossbauer spectra for CoFe₂O₄ determined that $\tilde{J} = 22 - 23$ K. There is a good quantitative coincidence with our result (11). Inserting (8) and (11) into (10), finally we have $J(Fe^A - Co^B) = 14.74$ K.

In analogy we obtain for the rest $MeFe_2O_4$ ($Me = Ni, Cu, Co, Mn$) compounds the results given in Table 2 where the anisotropy constants D of the different doping ions are taken from the experimental data whereas the exchange constants J are calculated in the present paper

Table 2. Spin values of Me^{2+} -ions, exchange interaction constants $J(Fe^A - Fe^B)$, $J(Fe^A - Me^B)$ and magnetic anisotropy constants of bulk $MeFe_2O_4$

Me^{2+} -ion	$D(X^\alpha)$ (K)	S	$MeFe_2O_4$	$J(Fe^A-Fe^B)$ (K)	$J(Fe^A-Me^B)$ (K)
Mg^{2+}	-0.12	0	$MgFe_2O_4$	33,78	-
Ni^{2+}	-0.69	1	$NiFe_2O_4$	33,78	31,38
Cu^{2+}	-0.47	1/2	$CuFe_2O_4$	33,78	24,96
Co^{2+}	4,68	3/2	$CoFe_2O_4$	33,78	14,74
Mn^{2+}	-0.22	5/2	$MnFe_2O_4$	33,78	12,18
Fe^{3+}	-0.87	5/2	-	-	-

We assume that $J(Fe^B - Me^B) = -0.1J(Fe^A - Me^B)$. Combining Table 1 and 2 we can determine the values of the exchange interactions for each compound and each concentration of Zn non-magnetic ions in the bulk system.

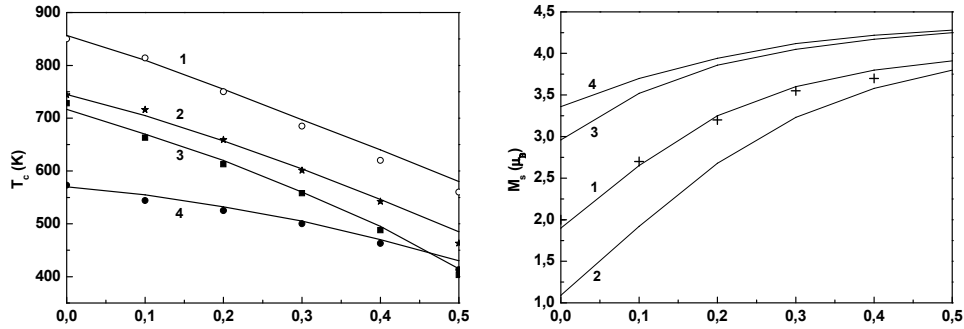


Fig. 1. T_C as a function of the Zn-concentration x for bulk: 1) $NiFe_2O_4$; 2) $CuFe_2O_4$; 3) $CoFe_2O_4$ and 4) $MnFe_2O_4$ for $J_b(X^\alpha - X^\beta)$ and $D_b(X^\alpha)$ given in TABLES I and II. The symbols denote the experimental data: \bullet – $MnFe_2O_4$; \blacksquare – $CoFe_2O_4$; $*$ – $CuFe_2O_4$ and \circ – $NiFe_2O_4$.

Fig. 2. M_s as a function of the Zn-concentration x for bulk: 1) $NiFe_2O_4$; 2) $CuFe_2O_4$; 3) $CoFe_2O_4$ and 4) $MnFe_2O_4$ for $J_b(X^\alpha - X^\beta)$ and $D_b(X^\alpha)$ given in TABLES I and II for $T = 300$ K. The symbols “+” correspond to the experimental data for $NiFe_2O_4$.

First, we present numerical calculations for the dependency of the transition temperature T_C and the saturation magnetization M_S on the doping concentration x ($0 \leq x \leq 0.4 - 0.5$) for bulk $Me_{1-x}Zn_xFe_2O_4$ ($Me = Ni, Co, Mn, Cu$) spinels (see Figures 1, 2). This allows us to test the proposed model and identify samples for mixed ferrite NPs.

With the increase of x the critical temperature T_C decreases for all mixed spinels. There is a good agreement between our theoretical results and the experimental data [1–4, 7, 8] which is an indirect evidence for the validity of our calculations and approximations.

To summarize: (i) A comparison of the numerical calculations with the experimental results demonstrates that within the given task, our model choice is suitable. (ii) Increase of the Zn-ion concentration leads to a simultaneous decrease of T_C , H_C and an increase in M_S .

In the case of MHT for *in vivo* applications the critical size of NPs does not exceed 20 – 25 nm. It is well known that the magnetic properties of NPs vary widely compared to bulk materials. The so called “size and surface effects” (see Fig. 3 and 4) lead to changes of the magnitude of the exchange interaction, magnetic anisotropy, and lattice constants on the surface compared to the bulk. The additions of Zn ions can induce compressive stress due to its larger ionic radius compared to the *Me* ions. In order to explain the decrease of T_C with decreasing particle size we consider the case $J_s < J_b; D_s < D_b$.

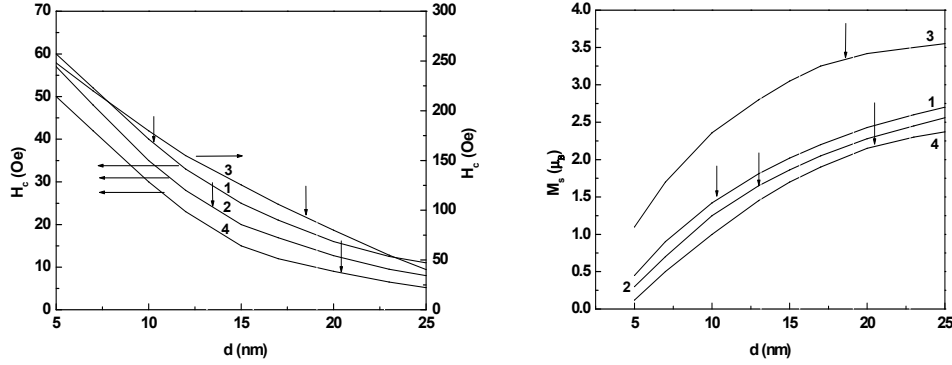


Fig. 3. Size dependence of the coercivity H_c for different NPs: 1) $\text{Ni}_{0.5}\text{Zn}_{0.5}\text{Fe}_2\text{O}_4$; 2) $\text{Cu}_{0.6}\text{Zn}_{0.4}\text{Fe}_2\text{O}_4$; 3) $\text{Co}_{0.6}\text{Zn}_{0.4}\text{Fe}_2\text{O}_4$ and 4) $\text{Mn}_{0.5}\text{Zn}_{0.5}\text{Fe}_2\text{O}_4$ for $J_s(X^\alpha - X^\beta) = 0.7J_b(X^\alpha - X^\beta)$ and $D_s(X^\alpha) = 0.8D_b(X^\alpha)$ given in Table 1 and 2 for $T = 0.65T_C$. Vertical arrows “↓” indicate the position of the optimal sizes of NPs with $T_C = 315$ K which are suitable for MHT.

Fig. 4. Size dependence of the magnetization M_s for different NPs: 1) $\text{Ni}_{0.5}\text{Zn}_{0.5}\text{Fe}_2\text{O}_4$; 2) $\text{Cu}_{0.6}\text{Zn}_{0.4}\text{Fe}_2\text{O}_4$; 3) $\text{Co}_{0.6}\text{Zn}_{0.4}\text{Fe}_2\text{O}_4$ and 4) $\text{Mn}_{0.5}\text{Zn}_{0.5}\text{Fe}_2\text{O}_4$ for $J_s(X^\alpha - X^\beta) = 0.7J_b(X^\alpha - X^\beta)$ and $D_s(X^\alpha) = 0.8D_b(X^\alpha)$ given in Table 1 and 2 for $T = 0.65T_C$. Vertical arrows “↓” indicate the position of the optimal sizes of NPs with $T_C = 315$ K which are suitable for MHT.

4. Conclusions

We have proposed a microscopic model which allows us to identify particles with structure formulas $\text{Co}_{0.6}\text{Zn}_{0.4}\text{Fe}_2\text{O}_4$, $\text{Cu}_{0.6}\text{Zn}_{0.4}\text{Fe}_2\text{O}_4$, $\text{Mn}_{0.5}\text{Zn}_{0.5}\text{Fe}_2\text{O}_4$ and $\text{Ni}_{0.5}\text{Zn}_{0.5}\text{Fe}_2\text{O}_4$ appropriated for *in vivo* MHT application. Using a Green’s function technique, we have calculated the magnetic properties of these compounds which are given in Table 3.

We obtain a good agreement with the experimental data. For example the maximum magnetization M and minimum coercive field H_c have been observed experimentally by t al. [4] in $\text{Co}_{1-x}\text{Zn}_x\text{Fe}_2\text{O}_4$ for $x = 0.4$ and the maximum M by Corral-Flores et al. [8] in $\text{Ni}_{1-x}\text{Zn}_x\text{Fe}_2\text{O}_4$ for $x = 0.5$, in agreement with our results (see Table 3). The concentration $x = 0.5$ observed in $\text{Mn}_{1-x}\text{Zn}_x\text{Fe}_2\text{O}_4$ is experimentally also confirmed by many authors [9, 10]. Moreover, the obtained value of $H_c = 40$ Oe for $\text{Ni}_{0.5}\text{Zn}_{0.5}\text{Fe}_2\text{O}_4$ NPs (see TABLE 3) is in a good quantitative coincidence with that of 42.2 Oe reported by Kozłowski [12].

Table 3. The calculated magnetic quantities M_S and H_C for different NPs with structure formula $Me_{1-x}Zn_xFe_2O_4$ appropriated for *in vivo* MHT application.

$Me_{1-x}Zn_xFe_2O_4$	$T_c(K)$	$d(nm)$	$M_S(\mu_B)$	$H_C(Oe)$
$Co_{0.6}Zn_{0.4}Fe_2O_4$	315	17.05	3.25	92.86
$Ni_{0.5}Zn_{0.5}Fe_2O_4$	315	11.36	1.50	40.00
$Cu_{0.6}Zn_{0.4}Fe_2O_4$	315	13.26	1.67	24.17
$Mn_{0.5}Zn_{0.5}Fe_2O_4$	315	20.00	2.11	9.17

LITERATURE

1. A. Franco, Jr. and F. C. de Silva. J. Appl. Phys. **113**, 17B513 (2013).
2. M. Rahimi, P. Kameli, M. Ranjbar, H. Hajhashemi, and H. Salamati. J. Mater. Sci. **48**, 2969 (2013).
3. T. Anjaneyulu, A. T. Raghavender, K. V. Kumar, P. N. Murthy, and K. Narendra. Ind. J. Res. **2**, 310 (2013).
4. Z. Beji, A. Hanini, L.S. Smiri, J. Gavard, K. Kacem, F. Villain, J.-M. Greneche, F. Chau, and S. Ammar. Chem. Mater. **22**, 5420 (2010).
5. A. T. Apostolov, I. N. Apostolova, and J. M. Wesselinowa. J. Appl. Phys. **109**, 083939 (2011).
6. I. Nowik. J. Appl. Phys. **40**, 872 (1969).
7. P. G. Bercoff and H. R. Bertorello. J. Mang. Mang. Mater **213**, 56 (2000).
8. M. Rahimi, P. Kameli, M. Rajbar, H. Hejhashemi, and H. Salamati. J. Mater. Sci. **48**, 2696 (2013).
9. K. S. Lohar, S. M. Patange, S. E. Shirsath, V. S. Surywansh, S. S. Gaikwad, S. S. Jadhav, and N. Kulkarni. Int. J. Adv. Eng. and Techn. **3**, 354 (2012).
10. S. A. Mazen, S. F. Mansour, and H. M. Zaki. Cryst. Res. Technol. **38**, 471 (2003).
11. E. De. Grave, R. M. Persoons, R. E. Vanderberghe, and P. M. A. de Bakker. Phys. Rev. B **47**, 5881 (1993).
12. G. Kozlowsky. Wright State University, CORE Scholar, Magnetic Nanoparticles in Hyperthermia Treatment, Special Session 5: Carbon and Oxide Based Nanostructured Materials (2012).

ФЕРИМАГНИТНИ НАНОЧАСТИЦИ ЗА САМОСЪГЛАСУВАНА МАГНИТНА ХИПЕРТЕРМИЯ (ФИЗИЧНИ АСПЕКТИ)

А. Т. Апостолов¹, И. Н. Апостолова²

Ключови думи: феритни наночастици, магнитна хипертермия

Научна област: физични науки, физика на твърдото тяло

РЕЗЮМЕ

На базата на модела на Хайзенберг, с включена в него еднородна анизотропия и използване на метода на функциите на Грин ние изследваме размерните и примесните ефекти върху температурата на Кюри (T_C), намагнитването на насищане (M_S) и коерцитивността (H_C) за сферични наночастици със структурна формула $Me_{1-x}Zn_xFe_2O_4$, където $Me = Ni, Cu, Co, Mn$. Показано е, че за $x = 0,4 - 0,5$ и $d = 10 - 20$ nm тези наночастици имат температура на фазовия преход $T_C = 315$ K, което ги прави подходящи за самоконтролирана магнитна хипертермия.

¹ Ангел Апостолов, доц. д-р, кат. „Физика“, УАСГ, бул. ”Хр. Смирненски № 1, 1046 София, e-mail: angelapos@abv.bg

² Илиана Апостолова, доц. д-р, кат. „Математика и физика“, Лесотехнически университет, бул. „Кл. Охридски“ 10, 1756 София, e-mail: inaapos@abv.bg

